# Minimizing ion competition boosts volatile metabolome analysis by secondary electrospray ionization orbitrap mass spectrometry

**Jérôme Kaeslin**[1 2], **Jiayi Lan**[1 2] & **Renato Zenobi**[1]

[1] Department of Chemistry and Applied Biosciences, ETH Zurich, Zurich, Switzerland

[2] Equal contribution, alphabetical order.

E-mail: `zenobi@org.chem.ethz.ch`

July 2020

**Abstract.** Secondary electrospray ionization high-resolution mass spectrometry (SESI-HRMS) is an emerging technique for detection of volatile metabolites. However, reduced sensitivity and reproducibility of SESI-HRMS have limited its applications in untargeted metabolomics profiling. Ion suppression in the SESI source has been considered to be the main cause. Here, we show that besides ion suppression, ion competition in the detection process on Orbitrap instruments is another important factor influencing sensitivity and reproducibility of SESI-MS. Instead of acquiring the full $m/z$ range, acquisition of consecutive $m/z$ windows to minimize the ion competition effect allows the detection of many more robust features. Optimal $m/z$ window ranges are proposed for measuring human breath and bacteria culture samples on SESI-Orbitrap MS, considering the balance for maximizing scanning speed and minimizing ion competition.

## 1. Introduction

Volatile metabolites provide deep insight into metabolism. Various methods were developed for the analysis of volatile metabolites and are commonly applied in clinical research, mainly using gas chromatography-mass spectrometry (GC-MS) [1], proton-transfer-reaction mass spectrometry (PTR-MS) [2] and selected-ion flow-tube mass spectrometry (SIFT-MS) [3]. Over the last decades, secondary electrospray ionization (SESI) has emerged and been widely used to ionize metabolites in the gas phase. Given its good modularity [4], SESI can be coupled with various commercial mass spectrometers. Particularly attractive is the coupling with high-resolution mass spectrometers (HRMS) e.g. an Orbitrap. Previous studies have shown that coupling to such a high-resolution instrument offers greater selectivity in feature detection and simplify metabolites identification.[5][6] Besides the number of detected features and the resolving power, the reproducibility of the detected features is an important aspect and was

addressed in recent standardization studies.[7][8]

However, reproducibility and sensitivity might be impaired by ion suppression - an effect well known for classical electrospray methods when a large number of analytes is introduced into the ion source and competition for charge carriers takes place.[9] Besides ion suppression, a large number of ions is also problematic with regards to space charge effects in ion trap based instruments which might deteriorate mass accuracy[10] and sensitivity[11] - an effect sometimes referred to as ion competition. These drawbacks can be minimized by a strategy called *spectral stitching* where smaller $m/z$ windows are acquired and stitched together instead of acquiring the whole $m/z$ range in one scan.[11][12] In the case of an Orbitrap, this avoids that the C-trap is overfilled with the most abundant ions while low abundant ions eventually are not accumulated long enough to be detected. However, spectral stitching has a significantly longer duty cycle than a full MS scan because many scans have to be acquired to complete a full spectrum. Instead of equal size $m/z$ windows, optimized $m/z$ window positions and widths were recently shown to enhance sensitivity while keeping the duty cycle short.[13]

Here, we apply that the same strategy as described in [13] to SESI-MS to minimize the effect of ion competition during data acquisition, where the duty cycle is very important because the events monitored are time-limited, for example, an exhalation lasts only a few seconds.

## 2. Methods

### *2.1. Real-time SESI-HRMS measurements of breath and bacteria cultures*

The SESI-HRMS system used consisted of a Super SESI source (Fossiliontech, Spain), an Exhalion flow sensor (Fossiliontech) and an Orbitrap Q-Exactive mass spectrometer (Thermo Scientific, San Jose, CA). A 20 $\mu$m non-coated TaperTip emitter (New Objective, Woburn, MA) was used for electrospray using an aqueous solution of 0.1% formic acid. The sampling line temperature of the SESI source was set to 130 °C and the ion chamber temperature was set to 90 °C. Breath was directly introduced into the sampling line and the ion chamber of the SESI source through a spirometry filter (MicroGard, Vyaire Medical, USA; 3 cm ID) as previously described [7]. By controlling the exhaust mass flow of the SESI source at 0.65 L/min and the nitrogen mass flow through the source at 0.35 L/min, flow of breath of 0.3 L/min was constantly sampled by the mass spectrometer. For bacteria culture, 0.3 L/min nitrogen was used as carrier gas, humidified, then flushed through a culture flask and introduced into the SESI source.

Data were acquired on the Orbitrap Q-Exactive system in profile mode. For both positive and negative mode acquisition, an ion transfer tube temperature of 250 °C, a

resolution of 140,000 at $m/z = 200$ for the Orbitrap, a $m/z$ scan range from 50 to 500, RF lens set at 55 %, and a maximum injection time of 100 ms were used. The automatic gain control (AGC) target, which regulates the number of ions accumulated in the C-trap and later injected into the Orbitap analyzer, was set to $5 \times 10^6$. As instrument blank, data were acquire without introducing human breath or bacteria culture head space. In parallel of the MS data acquisition, the $CO_2$%, pressure, flow rate and total volume of the gas flows into the SESI source were measured by the Exhalion flow sensor.

Multiple MS acquisition methods with different scan ranges were used, including i) full scan in range from 50 to 500 m/z ; (ii) targeted with the narrowest scan window possible from 204.8 to 205.2 $m/z$ ; iii) twenty-two 20 $m/z$ windows with an overlap of 4 $m/z$ ; iv) six windows covering the 50 to 500 $m/z$ range splitted either according to the equal-feature number criterion (equal number of robust features per window - the same strategy as in [13]) or the equal-cumulative intensity criterion (equal accumulated intensity per window), with an overlap of 1 $m/z$. Figure 1(a) shows how these ranges are allocated while a subject is exhaling.

### *2.2. Data processing*

Raw data generated from the mass spectrometer were first converted into .mzXML format via MSConvert (ProteoWizard [14]). The converted files were then be imported into Matlab (version R2019b, MathWorks, Natick, MA) and treated using a Matlab code developed in-house. Briefly, $m/z$ peaks were picked from an overall averaged spectrum of acquired spectra during the experiment. The acquired data were then centroided using the picked peaks, and a .csv file containing the intensities of the peaks per scan was generated for each of the acquired MS data.

Statistics and window suggestions were calculated using in-house developed R codes. The .csv files generated were first summarized into intensities of the peaks for each of the raw data (full scan data as the average of scans, spectra acquired with windows as the sum of all scans within one duty cycle, where for the overlaps between windows intensities were averaged). The peaks were grouped within 5 ppm error and the peak intensities were summed as the peak group intensity. The summed data were then used to identify robust features using the criteria as described by Sarvin et al. [13]. Briefly, a feature was considered "robust" only if it matches the following criteria: i) observed in $\geq 80$ % of the biological samples; ii) the median intensity of the biological samples is above 1000 units; iii) signal-to-noise ratio above 4; iv) for breath samples, relative standard deviation (RSD) across the biological sample injection lower than 30 % and for bacteria culture, lower than 100 %. The window suggestions were then given by either equal number of features per window, or equal cumulative intensity per window.

## 3. Results and discussion

### *3.1. Targeted data acquisition method improves sensitivity of SESI-HRMS*

In a classical SESI-MS study, full MS scans are acquired repeatedly to track a subject's exhalation (figure 1(a) on row i)). From this data, an averaged MS can be calculated (1(b) and (c)). Depicting a signal over time gives an idea whether the features is elevated during exhalation or not - as in the case of figure 1(d) where the feature was inconstantly detected by the mass spectrometer. Such features below a certain exhalation-to-background threshold can not be confidently quantified or attributed to the breath events. Consequently, they are typically filtered out during data analysis.[15]

Based on the hypothesis that ion competition might limit sensitivity and robustness in SESI-MS, we investigated how the feature detection performance is influence by the acquisition method and therefore by the extent the C-trap is filled with analytes of interest. Three exhalations were acquired with a full scan method from 50 - 500 $m/z$ and with a targeted method from 204.8-205.2 $m/z$ (rows i) and ii) in figure 1). More signals were observed in the region 204.8-205.2 $m/z$ with the targeted method (figure 1(c)). Additionally, the signals were clearly elevated during exhalation with the targeted method while the full scan method suffered from a poor exhalation-to-background ratio (exemplary time trace in figure 1(d)). The full scan method, which fills the C-trap with all available ions, performs significantly worse than the targeted method, which only traps the ions of interest. These observations support the hypothesis that ion competition limits sensitivity and robustness of the observed features. Similar results were found for other targeted mass ranges (89.8-90.2, 253.9-254.3, 397.9-398.3, 412-412.4 $m/z$, results not shown).

Our result suggests that ion competition limits the sensitivity on SESI-Orbitrap instruments. Therefore, we recommend to use a targeted method on SESI-Orbitraps when the molecular targets are available, and to minimize the ion competition effects in untargeted studies. Eventually, we proposed to use optimized $m/z$ windows to minimize ion competition, in order to reach a comparable sensitivity and robustness with untargeted SESI-HRMS as with a targeted approach. How to get to these optimized $m/z$ windows is addressed in the following sections.

### *3.2. Defining ion distribution of human breath and bacteria culture*

To obtain the feature detection of samples with minimized ion competition effect, a series of twenty-two 20 $m/z$ isolation windows were used to scan through the full mass range (50 - 500 $m/z$). The distribution of features and intensities is shown in figure 2 for the full scan method, with ion competition, and for the 22 windows method, with minimized ion competition. Comparing to the full scan method, a significant increase of

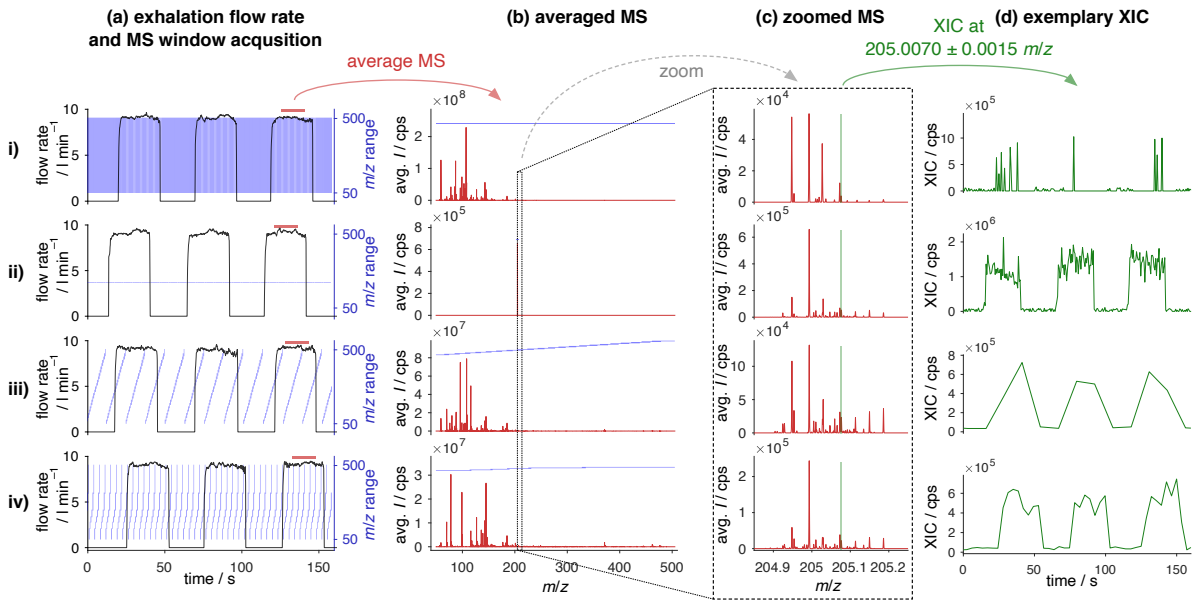


Figure 1: Overview of different acquisition strategies; i) full scan from 50 - 500 $m/z$; ii) targeted from 204.8 - 205.2 $m/z$; iii) 22 sequential 20 $m/z$ windows; iv) 6 optimized intensity windows: (a) shows three exhalations of a subject and plots the exhalation flow rate. The scan windows are shown in blue. (b) Shows the average spectrum during the last exhalation. (c) shows a zoom into the spectrum. (d) shows the XIC of an exemplary selected feature.

the number of robust features was observed in breath positive mode while minimizing the ion competition effect (920 in full scan and 2206 with 20 $m/z$ windows acquisition), but the robust features in negative mode were decreased (290 in full scan and 172 with 20 $m/z$ windows acquisition). In both polarities the method with 20 $m/z$ windows outperform the full scan method in the higher mass region ( $m/z \geq 200$ ), which matches exactly what we expected; that the dominating peaks in the low mass region are saturating the C-trap therefore reduce the overall detection sensitivity (figure 2 (c)). Reducing the ion competition with the 20 $m/z$ windows results in a similar feature distribution as observed on a SESI-quadrupole time-of-flight (QTOF) instrument[16] , where we assume that ion competition is less pronounced. Therefore, we conclude that a window splitting approach should be considered to make full use of the SESI's high mass ionization capabilities.

However, in negative mode, the 20 $m/z$ window method detected less robust features in the low mass region. In negative mode, the ion competition is less pronounced because no metabolite significantly dominates the ionization and detection process. Instead, the counting statistics become more important i.e. how reproducible a features is detected in a given time interval. Using the full scan method generates more scans over the whole mass range in a given time. Consequently, the features variation be-

comes lower and more features are classified as robust in negative mode full scan MS. Alternatively, the more abundant features in the low mass region in the full scan data could be attributed to ion fragmentation in the quadrupole or C-trap.

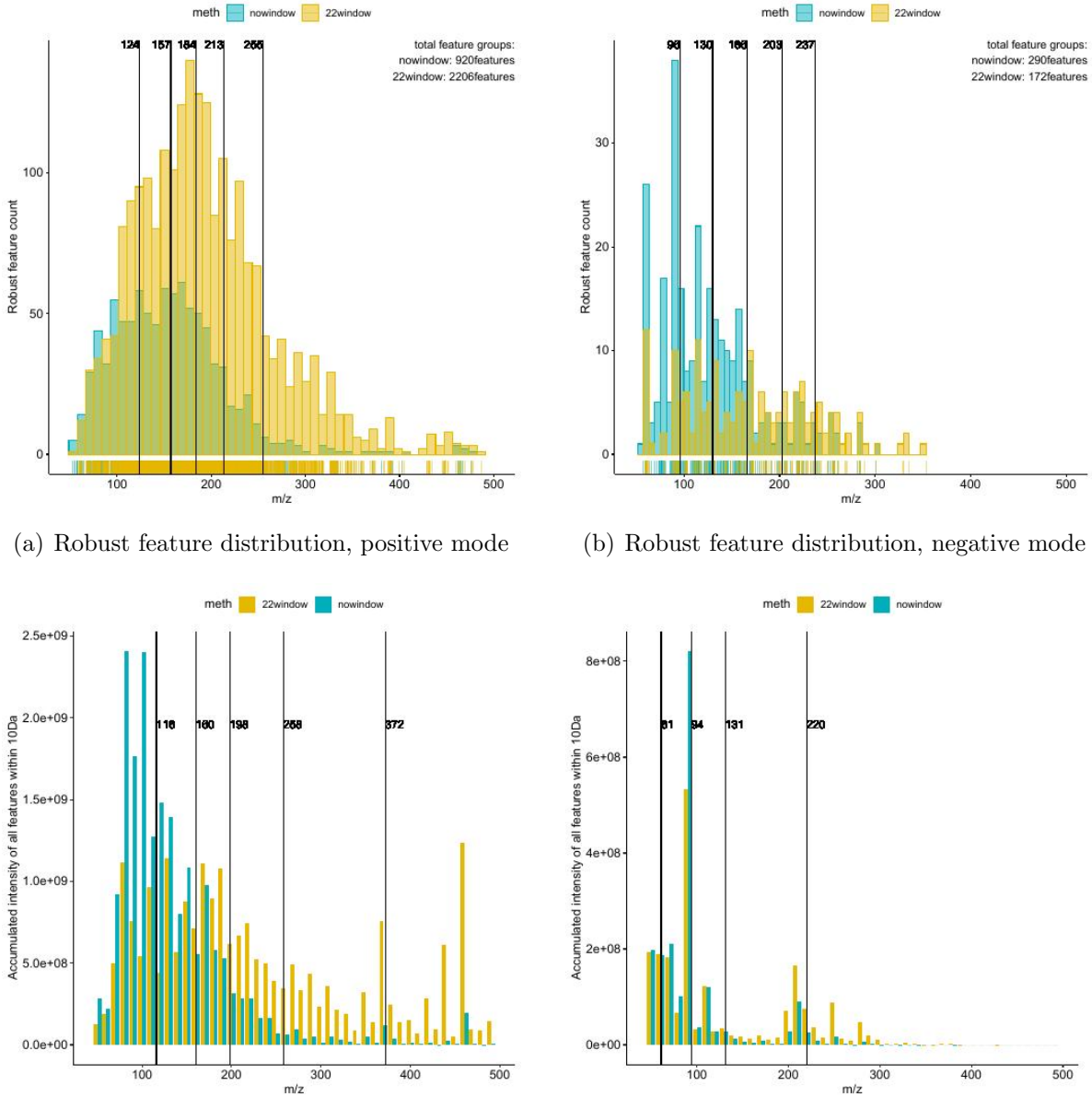


(a) Robust feature distribution, positive mode

(b) Robust feature distribution, negative mode

(c) Cumulative intensities, positive mode

(d) Cumulative intensities, negative mode

Figure 2: Robust feature distribution and cumulative intensities of all detected features within 10 $m/z$ over 50-500 $m/z$ range, of human breath volatiles.

The same approach was applied to bacteria culture samples. By minimizing the ion competition effect, a strong enhancement of feature detection were observed in both positive and in negative mode (figure 3). Highly intensive peaks were observed in low

mass region of both positive and negative mode, as shown in figure 3 (c) and (d).

While the 22 windows approach significantly enhances the number of observed features, it also increases the duty cycle. Figure 1 in row iii) shows one stitched full MS spectrum might be recorded only once or twice during the time of one exhalation and thus the time trace in figure 1d) is poorly resolved. With the aim to sample more data points in one exhalation while still preserving the enhanced sensitivity, we aimed to optimize the $m/z$ windows position and width.

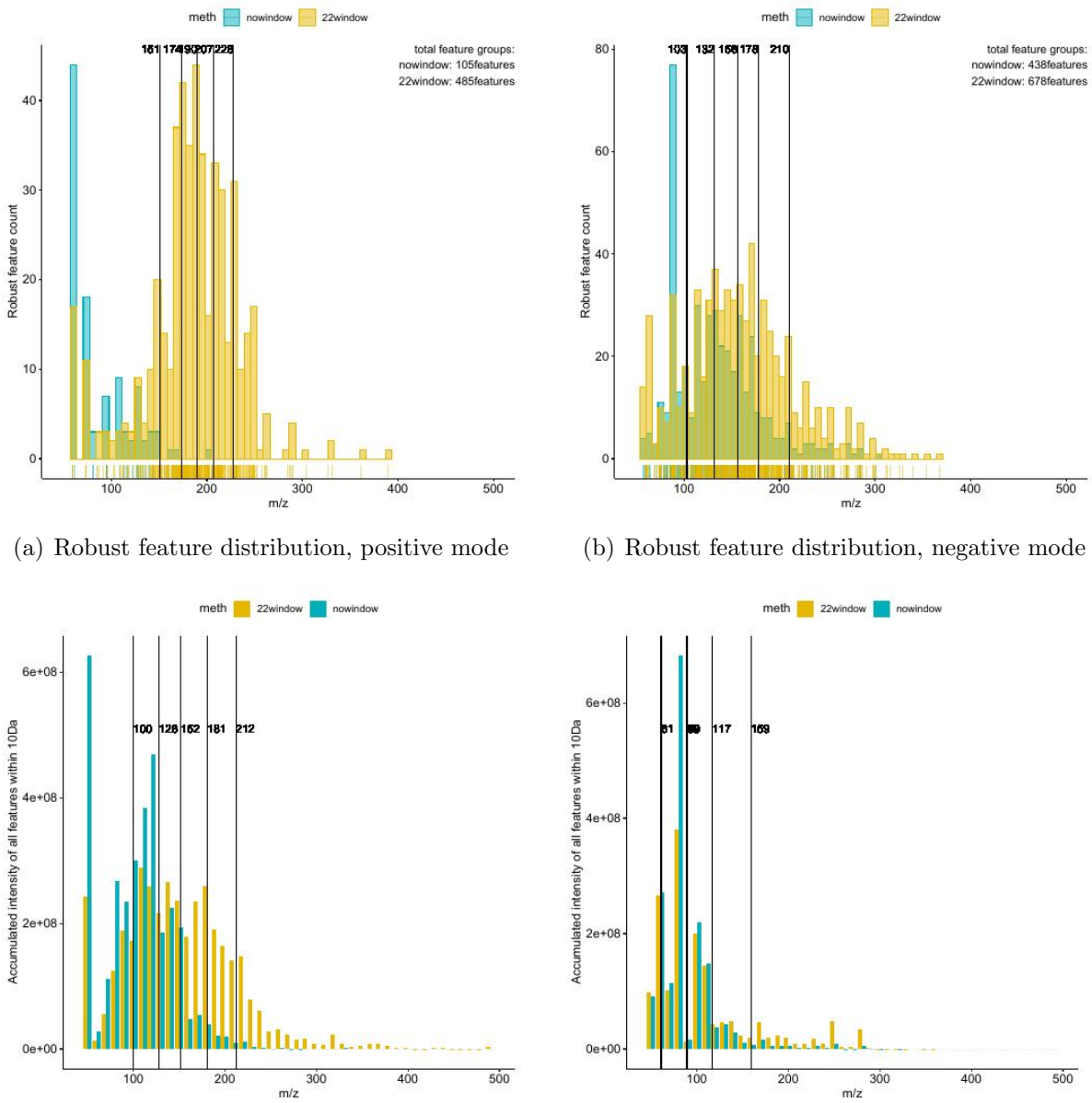


(a) Robust feature distribution, positive mode

(b) Robust feature distribution, negative mode

(c) Cumulative intensities, positive mode

(d) Cumulative intensities, negative mode

Figure 3: Robust feature distribution and cumulative intensities of all detected features within 10 $m/z$ over 50-500 $m/z$ range, of bacteria culture volatiles.

### *3.3. Optimized mass window for human breath and bacteria head space acquisition*

As a balance between short duty cycle and the windows number, 6 windows were selected and suggestions of window splitting were given for both human breath and for bacteria culture head space. ( $\sim$ 3 s per duty cycle at a resolution of 175'000 for the Orbitrap Q-Exactive Plus). More windows suggestions can be found in table S1 and S2 depending on the desired sampling frequency and thus the acceptable number of windows. Two approaches have been considered here to optimize the window splitting of the mass range. First, we split the complete mass range into windows containing an equal number of robust features as suggested by Sarvin et al.[13] Second, we split such that the windows contain an equal cumulative intensity of the robust features per window. For the second approach we hypothesize that it is the ion count leading to ion competition and not necessarily the number of features. As shown in figure 4, both methods yield in a similar number of robust features with the 22 windows methods (1862/387 for splitting according to feature numbers and 1779/362 for splitting according to intensities, positive/negative mode respectively). Noticeably, while using the intensity based windows for data acquisition, the ion competition effect was further eased in the low mass region comparing to the feature based windows, and this leads to a higher number of robust features, as show in figure 4 (a) and (b). While applying the same approaches to the bacteria culture samples, 223/393 for splitting according to feature numbers and 1036/1004 for splitting according to intensities, positive/negative mode respectively.

Again, we compared how the optimized 6 intensity windows perform compared to the full scan method, targeted method and 22 windows method when a subject exhales three times. Observing the exemplary feature at 205.0070 $m/z$, a clearly elevated signal is observed during exhalation in figure 1d) row iv). Consequently, the optimized 6 windows outperform the full scan method with regards to the detected feature and sensitivity ( figure 1d) row i)) and the 22 windows method in terms of duty cycle (figure 1d) row iii)) thus allowing to track the exhalation at multiple time points. Additionally, it is an untargeted approach and less limited by *a priori* knowledge compared to the targeted method (figure 1d) row ii)).

## 4. Conclusions

We show that ion competition indeed limits the sensitivity and robust feature detection for volatiles analysis with a SESI Orbitrap MS. For targeted applications, our findings show that a narrow $m/z$ window is superior to an untargeted full MS acqusition with regards to sensitive and robust feature detection. For untargeted studies, a sequential $m/z$ window acquisition enhances the sensitivity and robustness but limits the sampling frequency by a longer duty cycle. By optimizing the $m/z$ window's position and width, a compromise between sensitivity and duty cycle can be found. We demonstrate this

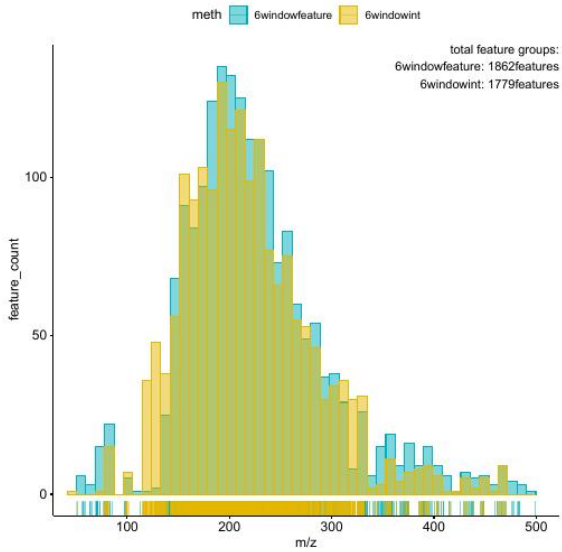


(a) Robust feature distribution, positive mode

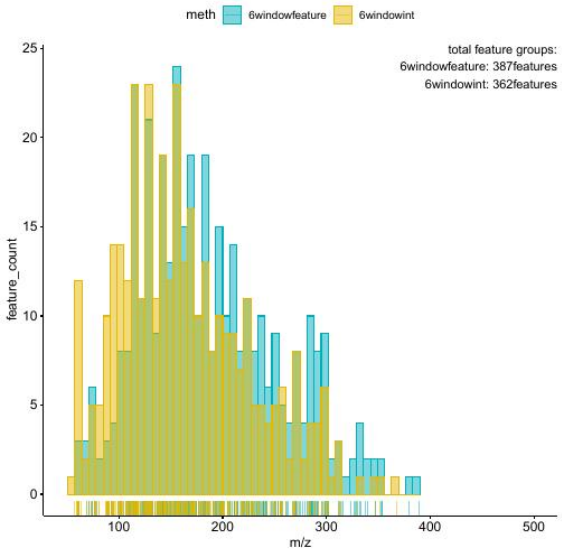


(b) Robust feature distribution, negative mode

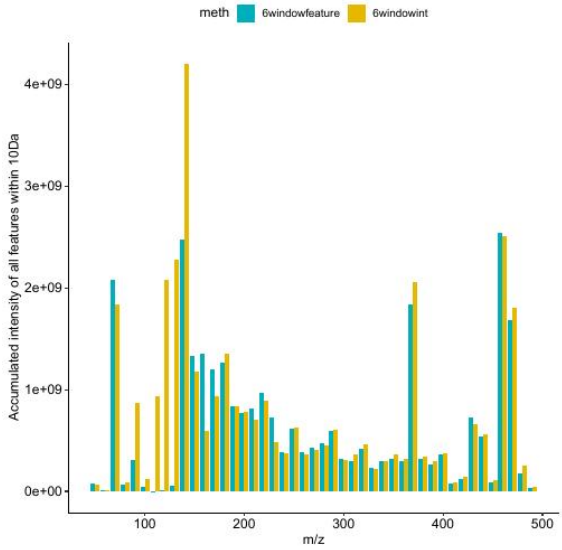


(c) Cumulative intensities (all features), positive mode

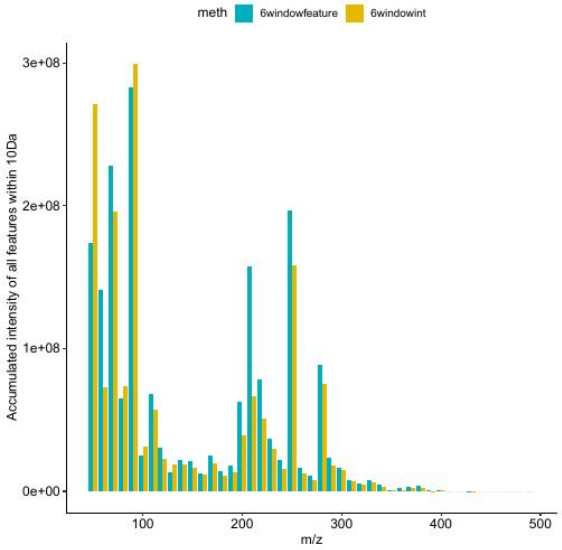


(d) Cumulative intensities (all features), negative mode

Figure 4: Human breath data acquired using optimized windows.

approach by using 6 optimized $m/z$ windows for the analysis of volatiles in breath and bacteria culture. An increase in sensitivity and robustness is observed while the duty cycle is still acceptable. Moreover, different sets of optimized windows for the analysis of breath or bacteria culture volatiles are proposed based on the feature number distribution or the cumulative intensity distribution.

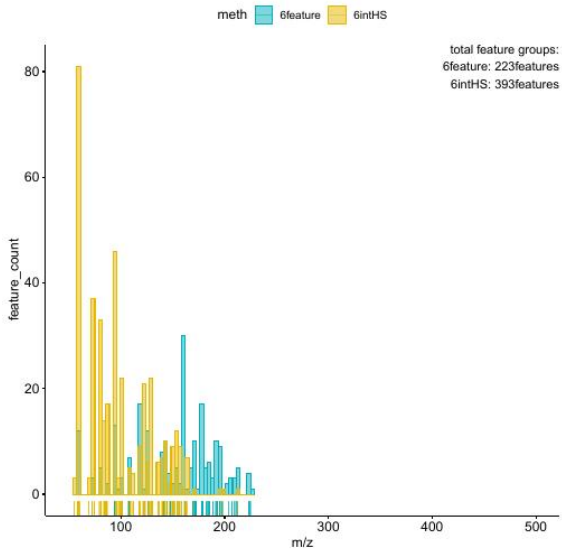


(a) Robust feature distribution, positive mode

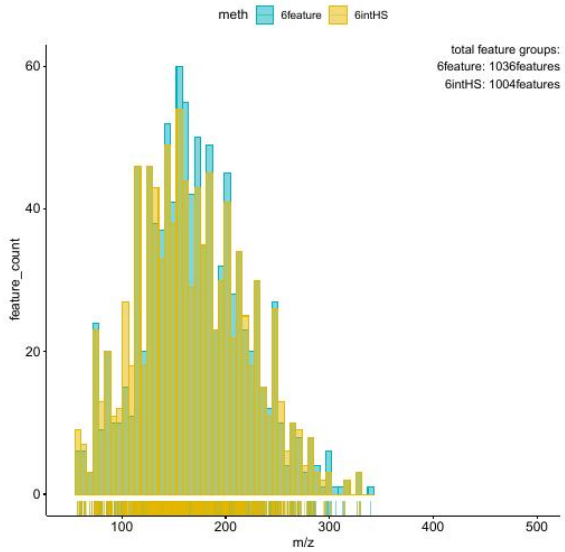


(b) Robust feature distribution, negative mode

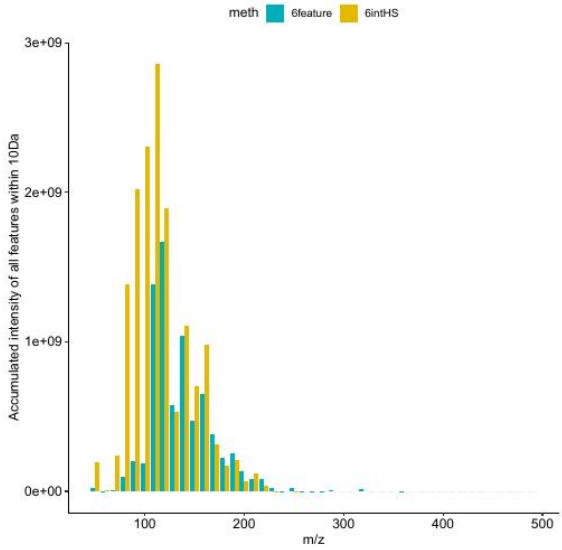


(c) Cumulative intensities (all features), positive mode

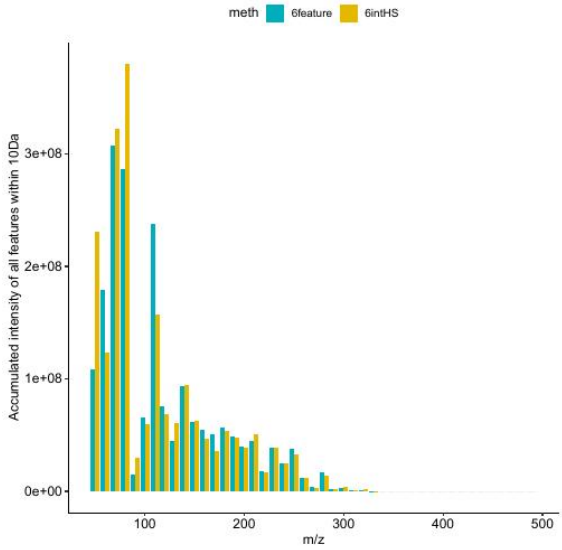


(d) Cumulative intensities (all features), negative mode

Figure 5: Bacteria culture head space measured using optimized windows.

## Acknowledgments

This work is part of the Zurich Exhalomics flagship project under the umbrella of "University Medicine Zurich/Hochschulmedizin Zürich".

**References**

[1] Changsong Wang, Ran Dong, Xiaoyang Wang, Ailing Lian, Chunjie Chi, Chaofu Ke, Lei Guo, Shanshan Liu, Wei Zhao, Guowang Xu, et al. Exhaled volatile organic compounds as lung cancer biomarkers during one-lung ventilation. *Scientific reports*, 4:7312, 2014.

[2] Phillip Trefz, Markus Schmidt, Peter Oertel, Juliane Obermeier, Beate Brock, Svend Kamysek, Jürgen Dunkl, Ralf Zimmermann, Jochen K Schubert, and Wolfram Miekisch. Continuous real time breath gas monitoring in the clinical environment by proton-transfer-reaction-time-of-flight-mass spectrometry. *Analytical chemistry*, 85(21):10321–10329, 2013.

[3] David Smith, Patrik vSpanvel, Beth Enderby, Warren Lenney, Claire Turner, and Simon J Davies. Isoprene levels in the exhaled breath of 200 healthy pupils within the age range 7–18 years studied using sift-ms. *Journal of breath research*, 4(1): 017101, 2009.

[4] Jiayi Lan, Francisco Blanco Parte, Guillermo Vidal-de Miguel, and Renato Zenobi. Secondary electrospray ionization. In *Breathborne Biomarkers and the Human Volatilome*, pages 185–199. Elsevier, 2020.

[5] Martin Thomas Gaugg, Diego Garcia Gomez, Cesar Barrios-Collado, Guillermo Vidal-de Miguel, Malcolm Kohler, Renato Zenobi, and Pablo Martinez-Lozano Sinues. Expanding metabolite coverage of real-time breath analysis by coupling a universal secondary electrospray ionization source and high resolution mass spectrometry—a pilot study on tobacco smokers. *Journal of breath research*, 10 (1):016010, 2016.

[6] Bertrand Rochat. From targeted quantification to untargeted metabolomics: Why lc-high-resolution-ms will become a key instrument in clinical labs. *TrAC Trends in Analytical Chemistry*, 84:151–164, 2016.

[7] Kapil Dev Singh, Georgi Tancev, Fabienne Decrue, Jakob Usemann, Rhea Appenzeller, Pedro Barreiro, Gabriel Jaumà, Miriam Macia Santiago, Guillermo Vidal de Miguel, Urs Frey, et al. Standardization procedures for real-time breath analysis by secondary electrospray ionization high-resolution mass spectrometry. *Analytical and bioanalytical chemistry*, pages 1–16, 2019.

[8] Jiayi Lan, Amanda Gisler, Tobias Bruderer, Pablo Sinues, and Renato Zenobi. Monitoring peppermint washout in the breath metabolome by secondary electrospray ionization-high resolution mass spectrometry. *Journal of breath research*, 2020.

[9] Thomas M Annesley. Ion suppression in mass spectrometry. *Clinical chemistry*, 49 (7):1041–1044, 2003.

[10] Li-Kang Zhang, Don Rempel, Birendra N Pramanik, and Michael L Gross. Accurate mass measurements by fourier transform mass spectrometry. *Mass Spectrometry Reviews*, 24(2):286–309, 2005.

[11] Andrew D Southam, Tristan G Payne, Helen J Cooper, Theodoros N Arvanitis, and Mark R Viant. Dynamic range and mass accuracy of wide-scan direct infusion nanoelectrospray fourier transform ion cyclotron resonance mass spectrometry-based metabolomics increased by the spectral stitching method. *Analytical chemistry*, 79(12):4595–4602, 2007.

[12] Andrew D Southam, Ralf JM Weber, Jasper Engel, Martin R Jones, and Mark R Viant. A complete workflow for high-resolution spectral-stitching nanoelectrospray direct-infusion mass-spectrometry-based metabolomics and lipidomics. *Nature protocols*, 12(2):310–328, 2017.

[13] Boris Sarvin, Shoval Lagziel, Nikita Sarvin, Dzmitry Mukha, Praveen Kumar, Elina Aizenshtein, and Tomer Shlomi. Fast and sensitive flow-injection mass spectrometry metabolomics by analyzing sample-specific ion distributions. *Nature Communications*, 11(1):1–11, 2020.

[14] Ravali Adusumilli and Parag Mallick. Data conversion with proteowizard msconvert. In *Proteomics*, pages 339–368. Springer, 2017.

[15] Martin Thomas Gaugg, Yvonne Nussbaumer-Ochsner, Lukas Bregy, Anna Engler, Nina Stebler, Thomas Gaisl, Tobias Bruderer, Nora Nowak, Pablo Sinues, Renato Zenobi, et al. Real-time breath analysis reveals specific metabolic signatures of copd exacerbations. *Chest*, 156(2):269–276, 2019.

[16] T Bruderer, MT Gaugg, L Cappellin, F Lopez-Hilfiker, M Hutterli, N Perkins, R Zenobi, and A Moeller. Detection of volatile organic compounds with secondary electrospray ionization and proton transfer reaction high-resolution mass spectrometry: A feature comparison. *Journal of the American Society for Mass Spectrometry*, 2020.

## Supplementary figures

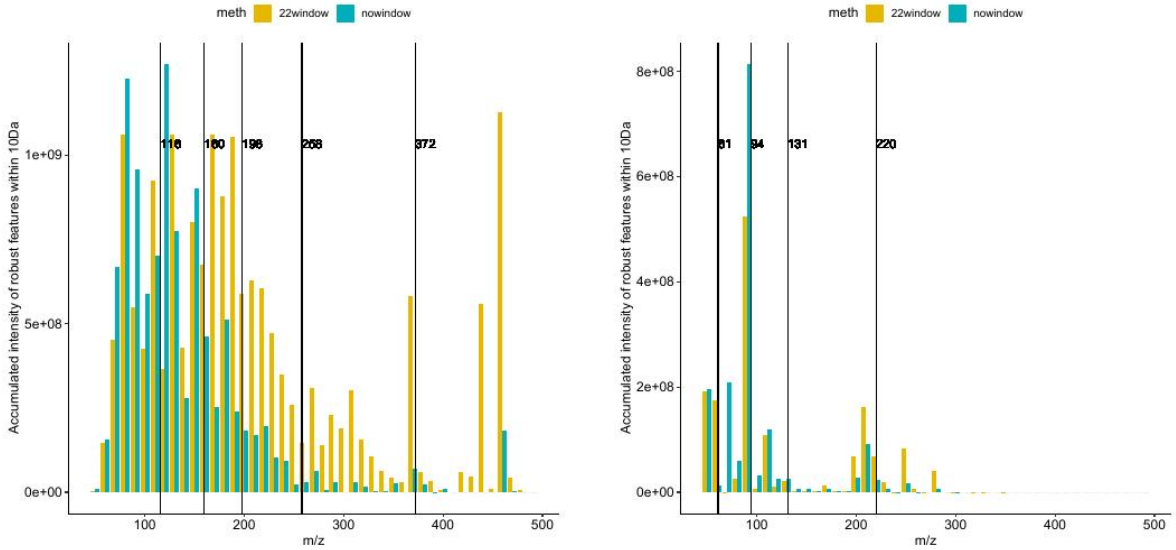


(a) Cumulative intensities, positive mode (b) Cumulative intensities, negative mode

Figure S1: Cumulative intensities of robust features within 10 $m/z$ over 50-500 $m/z$ range, of human breath volatiles, acquired using full scan method and 20 $m/z$ windows.

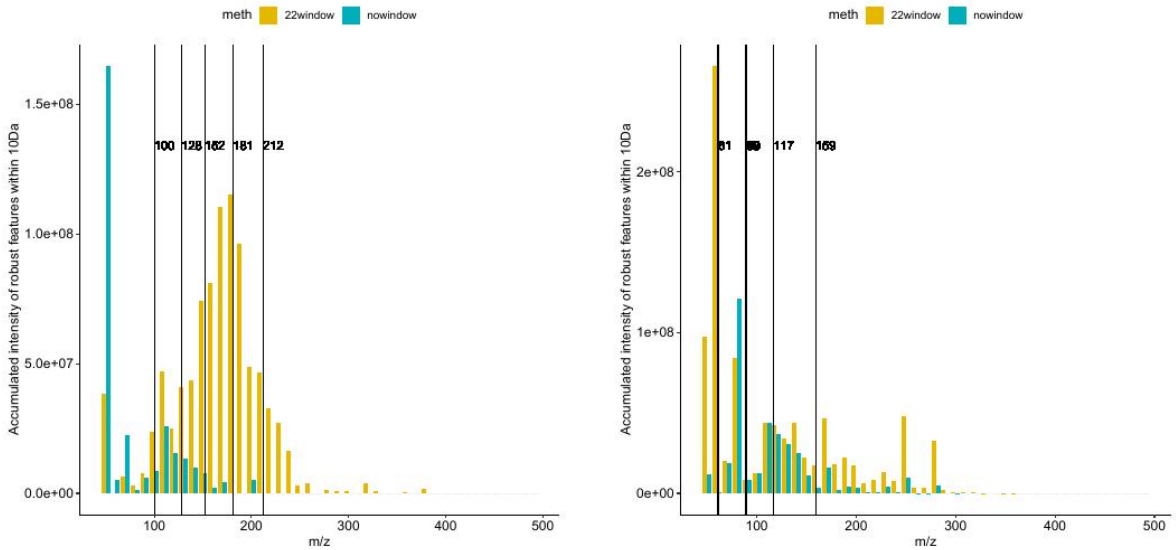


(a) Cumulative intensities, positive mode (b) Cumulative intensities, negative mode

Figure S2: Cumulative intensities of robust features within 10 $m/z$ over 50-500 $m/z$ range, of bacteria culture volatiles, acquired using full scan method and 20 $m/z$ windows.

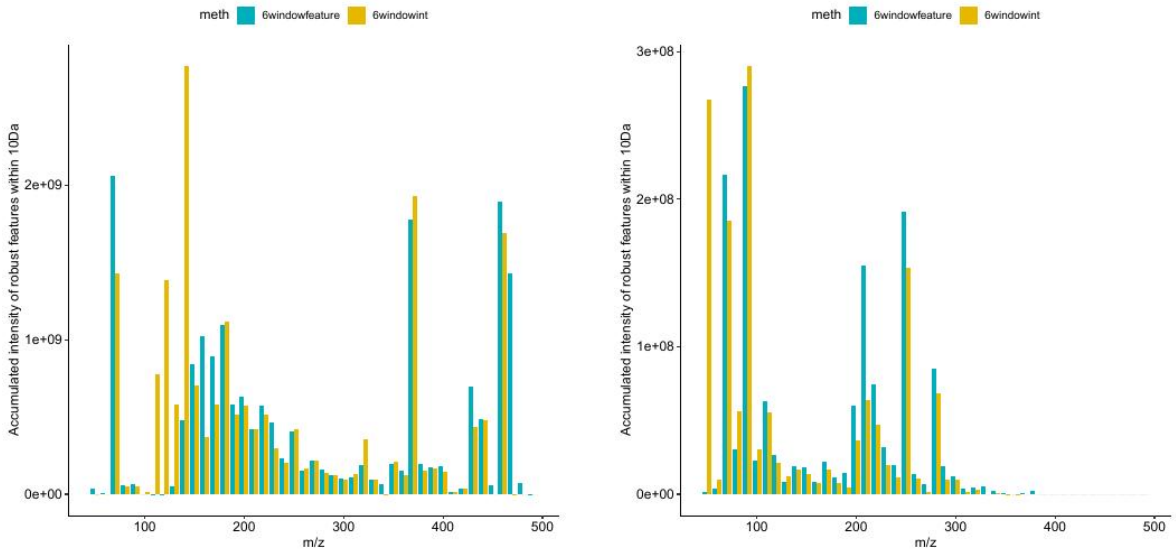


(a) Cumulative intensities (robust features), positive mode

(b) Cumulative intensities (robust features), negative mode

Figure S3: Cumulative intensities of robust features within 10 $m/z$ over 50-500 $m/z$ range, of bacteria culture volatiles, acquired using optimized windows.

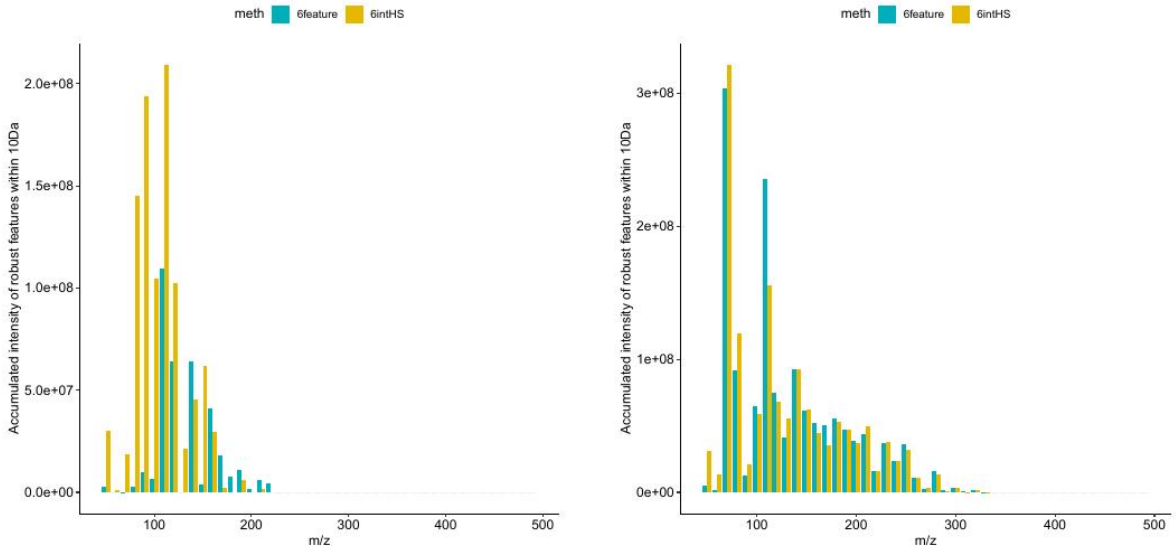


(a) Cumulative intensities (robust features), positive mode

(b) Cumulative intensities (robust features), negative mode

Figure S4: Cumulative intensities of robust features within 10 $m/z$ over 50-500 $m/z$ range, of bacteria culture volatiles, acquired using optimized windows.

Table S1: Optimized $m/z$ windows in positive mode for breath and for bacteria cultures. The reported windows were optimized to either contain an equal number of features or intensity. Different numbers $N$ of windows are proposed such that an analyst can find a compromise between sensitivity and duty cycle.

| | $N$ | 1 | 2 | 3 | 4 | 5 | 6 | 7 | 8 | 9 | 10 | 11 | 12 | 13 | 14 | 15 | 16 |
|---|---|---|---|---|---|---|---|---|---|---|---|---|---|---|---|---|---|
| + breath feature optimized | 2 | 50 – 184 | 183 – 500 | | | | | | | | | | | | | | |
| | 4 | 50 – 141 | 140 – 184 | 183 – 231 | 230 – 500 | | | | | | | | | | | | |
| | 6 | 50 – 124 | 123 – 157 | 156 – 184 | 183 – 213 | 212 – 255 | 254 – 500 | | | | | | | | | | |
| | 8 | 50 – 115 | 114 – 141 | 140 – 165 | 164 – 184 | 183 – 206 | 205 – 231 | 230 – 274 | 273 – 500 | | | | | | | | |
| | 10 | 50 – 110 | 109 – 131 | 130 – 152 | 151 – 170 | 169 – 184 | 183 – 200 | 199 – 220 | 219 – 245 | 244 – 291 | 290 – 500 | | | | | | |
| | 12 | 50 – 106 | 105 – 124 | 123 – 141 | 140 – 157 | 156 – 172 | 171 – 184 | 183 – 197 | 196 – 213 | 212 – 231 | 230 – 255 | 254 – 303 | 302 – 500 | | | | |
| | 14 | 50 – 101 | 100 – 119 | 118 – 133 | 132 – 150 | 149 – 162 | 161 – 174 | 173 – 184 | 183 – 195 | 194 – 209 | 208 – 224 | 223 – 241 | 240 – 268 | 267 – 311 | 310 – 500 | | |
| | 16 | 50 – 98 | 97 – 115 | 114 – 128 | 127 – 141 | 140 – 153 | 152 – 165 | 164 – 175 | 174 – 184 | 183 – 194 | 193 – 206 | 205 – 217 | 216 – 231 | 230 – 249 | 248 – 274 | 273 – 316 | 315 – 500 |
| + breath intensity optimized | 2 | 50 – 198 | 197 – 500 | | | | | | | | | | | | | | |
| | 4 | 50 – 137 | 136 – 198 | 197 – 305 | 304 – 500 | | | | | | | | | | | | |
| | 6 | 50 – 116 | 115 – 160 | 159 – 198 | 197 – 258 | 257 – 372 | 371 – 500 | | | | | | | | | | |
| | 8 | 50 – 101 | 100 – 137 | 136 – 173 | 172 – 198 | 197 – 239 | 238 – 305 | 304 – 406 | 405 – 500 | | | | | | | | |
| | 10 | 50 – 97 | 96 – 124 | 123 – 152 | 151 – 178 | 177 – 198 | 197 – 228 | 227 – 278 | 277 – 356 | 355 – 446 | 445 – 500 | | | | | | |
| | 12 | 50 – 88 | 87 – 116 | 115 – 137 | 136 – 160 | 159 – 180 | 179 – 198 | 197 – 224 | 223 – 258 | 257 – 305 | 304 – 372 | 371 – 447 | 446 – 500 | | | | |
| | 14 | 50 – 81 | 80 – 110 | 109 – 130 | 129 – 146 | 145 – 167 | 166 – 183 | 182 – 198 | 197 – 221 | 220 – 247 | 246 – 284 | 283 – 333 | 332 – 383 | 382 – 463 | 462 – 500 | | |
| | 16 | 50 – 81 | 80 – 101 | 100 – 119 | 118 – 137 | 136 – 155 | 154 – 173 | 172 – 183 | 182 – 198 | 197 – 219 | 218 – 239 | 238 – 272 | 271 – 305 | 304 – 361 | 360 – 406 | 405 – 463 | 462 – 500 |
| + HS feature optimized | 2 | 50 – 190 | 189 – 500 | | | | | | | | | | | | | | |
| | 4 | 50 – 167 | 166 – 190 | 189 – 241 | 240 – 500 | | | | | | | | | | | | |
| | 6 | 50 – 151 | 150 – 174 | 173 – 190 | 189 – 207 | 206 – 228 | 227 – 500 | | | | | | | | | | |
| | 8 | 50 – 140 | 139 – 167 | 166 – 178 | 177 – 190 | 189 – 199 | 198 – 214 | 213 – 233 | 232 – 500 | | | | | | | | |
| | 10 | 50 – 128 | 127 – 157 | 156 – 172 | 171 – 180 | 179 – 190 | 189 – 196 | 195 – 210 | 209 – 221 | 220 – 239 | 238 – 500 | | | | | | |
| | 12 | 50 – 113 | 112 – 151 | 150 – 167 | 166 – 174 | 173 – 181 | 180 – 190 | 189 – 194 | 193 – 207 | 206 – 214 | 213 – 228 | 227 – 246 | 245 – 500 | | | | |
| | 14 | 50 – 103 | 102 – 146 | 145 – 160 | 159 – 171 | 170 – 177 | 176 – 182 | 181 – 190 | 189 – 193 | 192 – 202 | 201 – 212 | 211 – 218 | 217 – 232 | 231 – 246 | 245 – 500 | | |
| | 16 | 50 – 88 | 87 – 140 | 139 – 153 | 152 – 167 | 166 – 173 | 172 – 178 | 177 – 183 | 182 – 190 | 189 – 193 | 192 – 199 | 198 – 208 | 207 – 214 | 213 – 226 | 225 – 233 | 232 – 248 | 247 – 500 |
| + HS intensity optimized | 2 | 50 – 152 | 151 – 500 | | | | | | | | | | | | | | |
| | 4 | 50 – 114 | 113 – 152 | 151 – 193 | 192 – 500 | | | | | | | | | | | | |
| | 6 | 50 – 100 | 99 – 128 | 127 – 152 | 151 – 181 | 180 – 212 | 211 – 500 | | | | | | | | | | |
| | 8 | 50 – 96 | 95 – 114 | 113 – 132 | 131 – 152 | 151 – 173 | 172 – 193 | 192 – 224 | 223 – 500 | | | | | | | | |
| | 10 | 50 – 83 | 82 – 110 | 109 – 124 | 123 – 138 | 137 – 152 | 151 – 170 | 169 – 186 | 185 – 203 | 202 – 228 | 227 – 500 | | | | | | |
| | 12 | 50 – 76 | 75 – 100 | 99 – 114 | 113 – 128 | 127 – 140 | 139 – 152 | 151 – 168 | 167 – 181 | 180 – 193 | 192 – 212 | 211 – 234 | 233 – 500 | | | | |
| | 14 | 50 – 74 | 73 – 97 | 96 – 111 | 110 – 119 | 118 – 130 | 129 – 142 | 141 – 152 | 151 – 165 | 164 – 176 | 175 – 188 | 187 – 200 | 199 – 216 | 215 – 240 | 239 – 500 | | |
| | 16 | 50 – 60 | 59 – 96 | 95 – 106 | 105 – 114 | 113 – 126 | 125 – 132 | 131 – 143 | 142 – 152 | 151 – 163 | 162 – 173 | 172 – 184 | 183 – 193 | 192 – 206 | 205 – 224 | 223 – 246 | 245 – 500 |

Table S2: Optimized $m/z$ windows in negative mode for breath and for bacteria cultures. The reported windows were optimized to either contain an equal number of features or intensity. Different numbers $N$ of windows are proposed such that an analyst can find a compromise between sensitivity and duty cycle.

| | $N$ | 1 | 2 | 3 | 4 | 5 | 6 | 7 | 8 | 9 | 10 | 11 | 12 | 13 | 14 | 15 | 16 |
|---|---|---|---|---|---|---|---|---|---|---|---|---|---|---|---|---|---|
| – breath feature optimized | 2 | 50 – 166 | 165 – 500 | | | | | | | | | | | | | | |
| | 4 | 50 – 117 | 116 – 166 | 165 – 221 | 220 – 500 | | | | | | | | | | | | |
| | 6 | 50 – 96 | 95 – 130 | 129 – 166 | 165 – 203 | 202 – 237 | 236 – 500 | | | | | | | | | | |
| | 8 | 50 – 93 | 92 – 117 | 116 – 132 | 131 – 166 | 165 – 190 | 189 – 221 | 220 – 251 | 250 – 500 | | | | | | | | |
| | 10 | 50 – 90 | 89 – 103 | 102 – 124 | 123 – 143 | 142 – 166 | 165 – 185 | 184 – 209 | 208 – 228 | 227 – 257 | 256 – 500 | | | | | | |
| | 12 | 50 – 80 | 79 – 96 | 95 – 117 | 116 – 130 | 129 – 145 | 144 – 166 | 165 – 184 | 183 – 203 | 202 – 221 | 220 – 237 | 236 – 262 | 261 – 500 | | | | |
| | 14 | 50 – 64 | 63 – 94 | 93 – 111 | 110 – 119 | 118 – 131 | 130 – 150 | 149 – 166 | 165 – 180 | 179 – 196 | 195 – 214 | 213 – 225 | 224 – 241 | 240 – 269 | 268 – 500 | | |
| | 16 | 50 – 62 | 61 – 93 | 92 – 103 | 102 – 117 | 116 – 125 | 124 – 132 | 131 – 152 | 151 – 166 | 165 – 173 | 172 – 190 | 189 – 208 | 207 – 221 | 220 – 231 | 230 – 251 | 250 – 271 | 270 – 500 |
| – breath intensity optimized | 2 | 50 – 94 | 93 – 500 | | | | | | | | | | | | | | |
| | 4 | 50 – 77 | 76 – 94 | 93 – 206 | 205 – 500 | | | | | | | | | | | | |
| | 6 | 50 – 61 | 60 – 94 | 93 – 94 | 93 – 131 | 130 – 220 | 219 – 500 | | | | | | | | | | |
| | 8 | 50 – 61 | 60 – 77 | 76 – 94 | 93 – 94 | 93 – 117 | 116 – 206 | 205 – 232 | 231 – 500 | | | | | | | | |
| | 10 | 50 – 61 | 60 – 77 | 76 – 90 | 89 – 94 | 93 – 94 | 93 – 117 | 116 – 172 | 171 – 220 | 219 – 252 | 251 – 500 | | | | | | |
| | 12 | 50 – 60 | 59 – 61 | 60 – 77 | 76 – 94 | 93 – 94 | 93 – 111 | 110 – 131 | 130 – 206 | 205 – 220 | 219 – 220 | 219 – 256 | 255 – 500 | | | | |
| | 14 | 50 – 60 | 60 – 61 | 60 – 61 | 60 – 77 | 76 – 89 | 88 – 94 | 93 – 94 | 93 – 103 | 102 – 119 | 118 – 194 | 193 – 220 | 219 – 221 | 220 – 256 | 255 – 500 | | |
| | 16 | 50 – 60 | 59 – 61 | 60 – 73 | 72 – 77 | 76 – 94 | 93 – 94 | 93 – 94 | 93 – 94 | 93 – 95 | 94 – 117 | 116 – 158 | 157 – 206 | 205 – 220 | 219 – 232 | 231 – 257 | 256 – 500 |
| – HS feature optimized | 2 | 50 – 156 | 155 – 500 | | | | | | | | | | | | | | |
| | 4 | 50 – 120 | 119 – 156 | 155 – 191 | 190 – 500 | | | | | | | | | | | | |
| | 6 | 50 – 103 | 102 – 132 | 131 – 156 | 155 – 178 | 177 – 210 | 209 – 500 | | | | | | | | | | |
| | 8 | 50 – 90 | 89 – 120 | 119 – 140 | 139 – 156 | 155 – 172 | 171 – 191 | 190 – 224 | 223 – 500 | | | | | | | | |
| | 10 | 50 – 88 | 87 – 113 | 112 – 129 | 128 – 143 | 142 – 156 | 155 – 170 | 169 – 184 | 183 – 201 | 200 – 234 | 233 – 500 | | | | | | |
| | 12 | 50 – 80 | 79 – 103 | 102 – 120 | 119 – 132 | 131 – 144 | 143 – 156 | 155 – 167 | 166 – 178 | 177 – 191 | 190 – 210 | 209 – 242 | 241 – 500 | | | | |
| | 14 | 50 – 75 | 74 – 95 | 94 – 115 | 114 – 128 | 127 – 136 | 135 – 145 | 144 – 156 | 155 – 165 | 164 – 174 | 173 – 186 | 185 – 199 | 198 – 214 | 213 – 251 | 250 – 500 | | |
| | 16 | 50 – 70 | 69 – 90 | 89 – 110 | 109 – 120 | 119 – 131 | 130 – 140 | 139 – 145 | 144 – 156 | 155 – 164 | 163 – 172 | 171 – 182 | 181 – 191 | 190 – 202 | 201 – 224 | 223 – 255 | 254 – 500 |
| – HS intensity optimized | 2 | 50 – 90 | 89 – 500 | | | | | | | | | | | | | | |
| | 4 | 50 – 76 | 75 – 90 | 89 – 126 | 125 – 500 | | | | | | | | | | | | |
| | 6 | 50 – 61 | 60 – 89 | 88 – 90 | 89 – 117 | 116 – 159 | 158 – 500 | | | | | | | | | | |
| | 8 | 50 – 61 | 60 – 76 | 75 – 89 | 88 – 90 | 89 – 102 | 101 – 126 | 125 – 178 | 177 – 500 | | | | | | | | |
| | 10 | 50 – 61 | 60 – 61 | 60 – 88 | 87 – 89 | 88 – 90 | 89 – 102 | 101 – 117 | 116 – 144 | 143 – 200 | 199 – 500 | | | | | | |
| | 12 | 50 – 61 | 60 – 76 | 75 – 89 | 88 – 89 | 88 – 90 | 89 – 102 | 101 – 117 | 116 – 126 | 125 – 159 | 158 – 212 | 211 – 500 | | | | | |
| | 14 | 50 – 61 | 60 – 61 | 60 – 61 | 60 – 86 | 85 – 89 | 88 – 89 | 88 – 90 | 89 – 102 | 101 – 103 | 102 – 117 | 116 – 134 | 133 – 172 | 171 – 234 | 233 – 500 | | |
| | 16 | 50 – 61 | 60 – 61 | 60 – 61 | 60 – 76 | 75 – 89 | 88 – 89 | 88 – 89 | 88 – 90 | 89 – 102 | 101 – 102 | 101 – 117 | 116 – 126 | 125 – 144 | 143 – 178 | 177 – 242 | 241 – 500 |